



# Improving single pass reduction during cold rolling by controlling initial texture of AZ31 magnesium alloy sheet

Di LIU, Zu-yan LIU, Er-de WANG

National Key Laboratory for Precision Hot Processing of Metals, School of Materials Science and Engineering, Harbin Institute of Technology, Harbin 150001, China

Received 21 October 2016; accepted 11 April 2017

**Abstract:** The AZ31 magnesium alloy sheets obtained by multi-pass hot rolling were applied to cold rolling and the maximum single pass cold rolling reduction prior to failure of AZ31 magnesium alloy was enhanced to 41%. Larger single pass rolling reduction led to weaker texture during the multi-pass hot rolling procedure. The sheet obtained showed weak basal texture, while the value was only 1/3–1/2 that of general as-rolled AZ31 Mg alloy sheets. It was beneficial for the enhancement of further cold rolling formability despite of the coarser grain size. The deformation mechanism for the formation of texture in AZ31 magnesium alloy sheet was also analyzed in detail.

**Key words:** AZ31 magnesium alloy; texture control; cold formability; work hardening

## 1 Introduction

Magnesium alloy sheets have attractive interests due to their excellent properties, as low density and high specific strength, making them potentially suitable candidates in automotive, aerospace and electronic industries [1]. Unfortunately, magnesium sheets usually exhibit poor ductility at room temperature [2] and the sheets must be rolled at elevated temperatures to avoid cracking which adds considerable cost of magnesium sheet products and is a significant impediment to their acceptance in industrial applications [3].

The poor cold rolling response of Mg is generally ascribed to its hexagonal crystallography and the associated lack of sufficient independent slip systems [4]. Usually, the single rolling pass reduction is less than 5% and the accumulative reduction of a rolling procedure is no more than 25% [5]. BARNETT et al [3] examined the cold rolling procedure of AZ31 magnesium alloy and the maximum cold rolling reduction achievable prior to failure was ~15%. CHANG et al [4] researched the texture and microstructure evolution of AZ31 Mg alloy, and the crack appeared when the cold rolling reduction reached 22%. These studies relied heavily on microstructure and texture of sheets after cold rolling. As

known, the cold rolling capacity of magnesium alloys closely depends on alloy composition, hot rolling technology and sheet microstructure. The maximum cold rolling reductions achievable of pure Mg, Mg–0.2Ce and Mg–3Al–1Zn prior to failure were ~30%, >90% and 15%, respectively [3]. However, practically no studies in the literature have focused on the influence of hot rolling technology and sheet microstructure on the further cold formability of AZ31 magnesium alloy sheets. In the present work, we emphasize texture control before cold rolling and its influence on cold formability. Therefore, the aim of the present work is to improve plastic deformation ability of initial cold rolling sheet by designing a reasonable hot rolling technology, so as to enhance the cold formability of AZ31 magnesium alloys.

## 2 Experimental

As-cast AZ31 magnesium alloy (Mg–2.85%Al–0.95%Zn) ingots with 26 mm in thickness were rolled to 2 mm in thickness through different rolling passes at a given reduction of ~15% (15 passes) or ~30% (7 passes) per pass by multi-pass hot rolling, and the obtained as-rolled sheets were named as sample A and sample B, respectively. The microstructure and room-temperature stress–strain curve of the initial ingot are shown in Fig. 1,

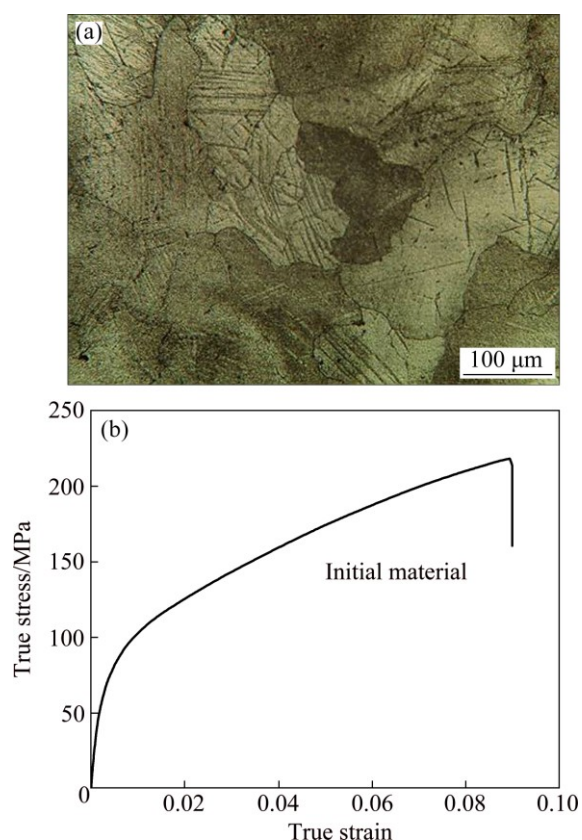


**Fig. 1** Microstructure (a) and room-temperature stress–strain curve (b) of initial material [6]

which were described in previous work [6].

The sheet thickness of each pass at the single pass reduction of 15% and 30% in the experimental procedure is shown in Table 1. In multi-pass hot rolling procedure, the starting temperatures of the sheets and rollers both were 400 °C. The temperature of the rollers was maintained at 400 °C using internal electric heaters and the sheets were no longer heated between passes. The temperature drop of the sheet between passes was kept at 15 °C. To implement the accurate control of rolling temperature, the time interval between passes was strictly controlled. The temperatures of the sheets before and after rolling were measured and recorded immediately at each pass. The samples were air cooled to room temperature and then applied to cold rolling. Cold rolling of the AZ31 magnesium alloy sheets was carried on the mill with a roll diameter of 190 mm and the rolling speed was 2 m/min. No heating was carried out during the cold rolling procedure. The specimens were cold rolled to different thickness reductions. The surface of the as-rolled sheets began to form cracks with the increasing of rolling reduction.

The microstructure and texture of the samples were identified using electron backscattered diffraction (EBSD) performed on a scanning electron microscope (SEM, Quanta 200 FEG-SEM) equipped with an EBSD detector

**Table 1** Sheet thickness of each pass at single pass reduction of 15% and 30% in experimental procedure

Procedure	Pass	Thickness/mm	
		15% reduction	30% reduction
Multi-pass hot rolling	Initial	26	26
	1	22.1	18.2
	2	18.8	12.7
	3	16	8.9
	4	13.6	6.2
	5	11.6	4.3
	6	9.9	3
	7	8.4	2 (Sample B)
	8	7.1	
	9	6	
	10	5.1	
	11	4.3	
	12	3.7	
	13	2.6	
	14	2.2	
15	2 (Sample A)		
Single-pass cold rolling	1	1.84	1.18

and OIM 6.14 analysis system. Surface preparation of the samples consisted of grinding with SiC emery papers of #200, #600, #800 and electrolytically polishing with solution of phosphoric acid and ethanol with a volume ratio of 3:5.

Tensile specimens with a gauge length of 25 mm and width of 6 mm were machined out of the samples along both RD and TD, where RD and TD are the rolling direction and transverse direction, respectively. Tensile tests were performed at room temperature using Instron 5569 testing machine at an initial strain rate of  $1.0 \times 10^{-3} \text{ s}^{-1}$ . To check the repeatability of the results, three experiments were conducted under each set of conditions.

### 3 Results and discussion

The schematic diagrams of rolling technology and stress analysis are shown in Fig. 2. During the rolling deformation, the sheet was mainly subjected to friction force ( $T$ ) along the rolling surface and the radial force ( $N$ ) perpendicular to rolling surface. Due to small contact arc and in order to analyze conveniently, the contact arc can approximately take as a plane,  $n$ -plane, seen in Fig. 2(b). In general, a variation in the rolling reduction has a significant influence on the bite angle  $\alpha$ , which is described as the central angle corresponding to the arc of the sheet contacting with the roller.

$$\cos \alpha = \frac{R - \frac{h_0 - h_f}{2}}{R} \quad (1)$$

where  $R$  is the roller radius,  $h_0$  and  $h_f$  are the initial and final sheet thickness, respectively. Take the first pass of hot rolling as example, the bite angles  $\alpha$  were  $11.6^\circ$  and  $16.5^\circ$  when the rolling reductions were 15% and 30%, respectively. In addition, the angle between radial force  $N$  and the normal direction of the sheet is defined as  $\varphi$ . In rolling procedure, the relationship between  $\alpha$  and  $\varphi$  can be described as

$$\varphi = \frac{\alpha}{K_x} \quad (2)$$

where  $K_x$  is the coefficient of resultant force point, and in stable rolling procedure,  $K_x \approx 2$ , indicating  $\varphi = \alpha/2$ .

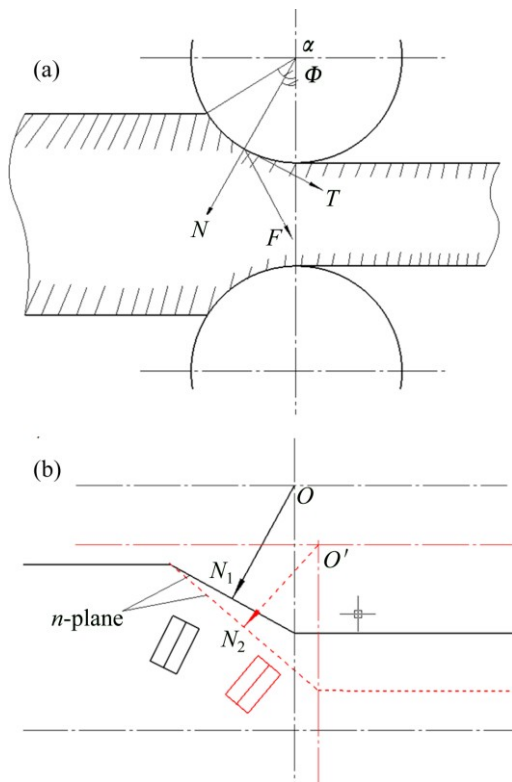


**Fig. 2** Schematic diagrams of rolling technology (a) and stress analysis (b)

The variation of bite angle will lead to different slopes of the  $n$ -plane as shown in Fig. 2(b). Under the influence of radial force  $N$ , basal slip impels grain rotation and  $\{0002\}$  basal plane rotates to perpendicular to radial force shown in Fig. 2. This makes a deviation angle form between basal plane of the grain and sheet plane, and it is the basic reason for the anisotropy of as-rolled sheet. When the initial sheet thickness is identical, the change of reduction has an influence on the bite angle (see the black line and red line in Fig. 2(b)), and further affects the angle between radial force and

normal direction, therefore, the basal texture intensity will change. As reported in AZ61 magnesium alloys [7], small angle variations are enough to change to predominant deformation mechanism during rolling, and further lead to the variation of texture characteristics.

Dislocation is multiplied with the deformation increasing, and leading to the growth of dislocation density. Therefore, the mutual reaction and delivery between dislocations is enhanced, and finally obstacles which impeding the movement of dislocations such as fixed delivery jog and dislocation pileup are produced, thus the work hardening degree is aggravated. When the rolling reduction increases or rolling temperature decreases, the grains are refined, the grain misorientations decrease and the grain boundaries increase. The movement is restricted in a certain range due to the impediment that dislocations fail to go through. This causes deformation resistance to increase and the continue deformation ability is significantly reduced. If the reduction is small or the temperature is high, the deformation resistance of each pass is corresponding small, the plastic deformation becomes uniform and is less likely to form strong texture, hence, the continue deformation ability is also improved. Therefore, the total deformation could be improved by designing a reasonable rolling procedure.

The hot rolled sheets obtained by multi-pass hot rolling procedure which were named as sample A and sample B were applied to cold rolling. The microstructures obtained by EBSD in the RD–TD plane of two samples are shown in Figs. 3(a) and (c), and the average grain sizes of the two samples were 4.7 and 16.8  $\mu\text{m}$ , respectively. Figures 3(b) and (d) both indicate that there is a peak distribution around  $30^\circ$  which corresponds to DRX grain boundaries [8].

Figures 4(a<sub>1</sub>) and (b<sub>1</sub>) display the  $\{0002\}$  pole figures of samples A and B obtained by EBSD data. The two samples both show a typical basal texture. The texture intensity can explain quantifiably by Schmid factor. Schmid factor  $m$  is defined as  $m = \cos \lambda \cos \phi$ , where  $\lambda$  is the angle between slip direction, e.g.  $\langle 11\bar{2}0 \rangle$  and the stress axis, and  $\phi$  is the angle between the normal of the slip plane, e.g.  $(0002)$  and the stress axis [9]. For single crystal, when  $\lambda = \phi = 45^\circ$ , there is a maximal value (0.5) of the Schmid factor, and the grain is easy to slip and plastic deformation is easy to occur by external force. While when  $\lambda$  or  $\phi$  equals  $90^\circ$ , there is a minimal value (0) of the Schmid factor, and in this condition, the grain cannot generate slip by external force. Thus, the average Schmid factor can be applied to representing the texture intensity for polycrystal. The Schmid factor maps of the two samples in RD and TD are shown in Figs. 4(a<sub>2</sub>), (a<sub>3</sub>), (b<sub>2</sub>) and (b<sub>3</sub>). The average Schmid factor of the two sheets in RD and TD were: 0.18 in RD and 0.14 in TD

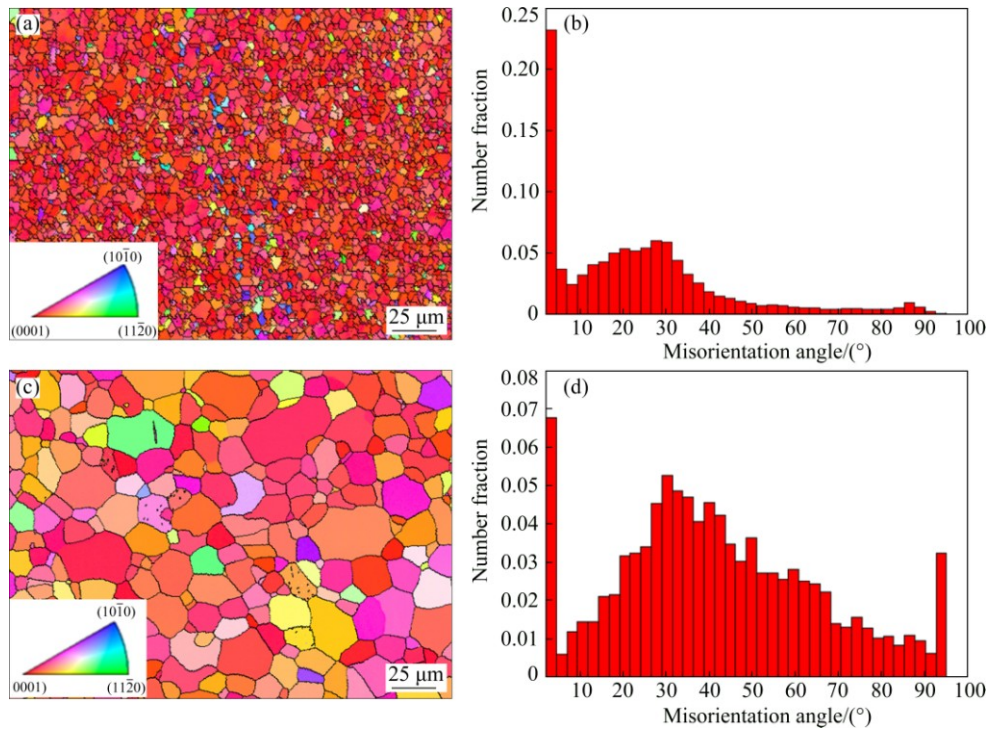


**Fig. 3** Inverse pole figure map (a, c) and misorientation angle distribution (b, d) of sample: (a, b) Sample A; (c, d) Sample B

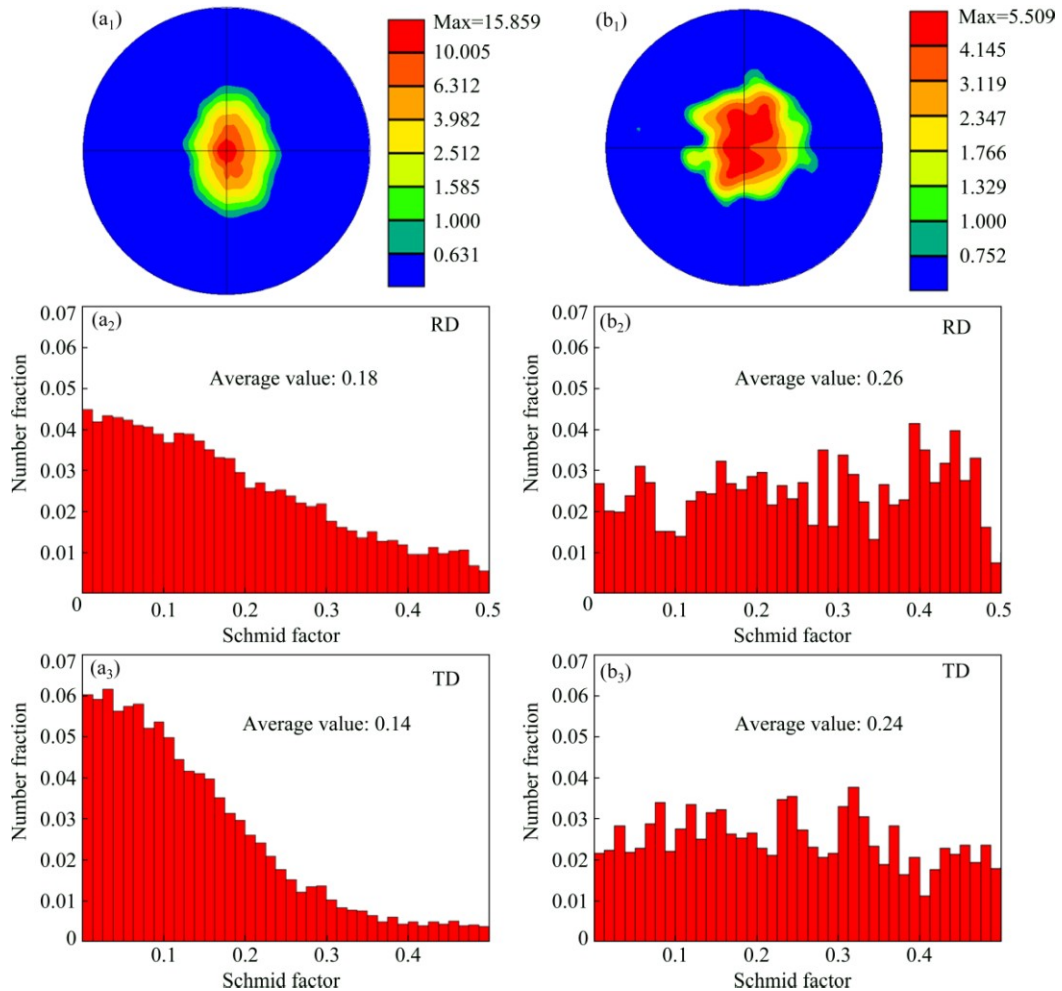


**Fig. 4** {0002} pole figures ( $a_1$ ,  $b_1$ ) and distributions of Schmid factor ( $a_2$ ,  $a_3$ ,  $b_2$ ,  $b_3$ ) in RD and TD of sample A ( $a_1$ ,  $a_2$ ,  $a_3$ ) and sample B ( $b_1$ ,  $b_2$ ,  $b_3$ )

for sample A, and 0.26 in RD and 0.24 in TD for sample B, respectively. In Figs. 4(a<sub>2</sub>) and (a<sub>3</sub>), the Schmid factor of most grains is below 0.3 suggesting that grain orientation is not favorable for basal slip. Thus, the {0002} basal texture intensity of sample A is much stronger than that of sample B.

The strong {0002} basal texture or near basal texture usually forms in rolling procedure of Mg alloys [10,11]. The formation of basal texture has a close correlation to basal slip [12]. Activation of basal slip during rolling deformation will progressively orient the basal planes of the grains parallel to the sheet plane [11]. The texture intensity is mainly influenced by rolling technology parameters such as rolling reduction and rolling temperature.

The room-temperature tension plots and hardening curves of samples A and B along RD and TD are presented in Fig. 5. The yield strength ( $\sigma_s$ ), ultimate tensile strength ( $\sigma_b$ ), elongation ( $\delta$ ) and work-hardening exponent ( $n$ ) of the two samples were summarized. The stress–strain curves exhibit that there are weaker strain hardening behavior and higher yield strength and ultimate tensile strength of sample A than sample B.

The hardening ability of plastic deformation is the key factor to decide the forming property. The plastic

deformation behavior of alloys can be explored by the flow equation describing the relationship between the true flow stress ( $\sigma$ ) and the true strain ( $\varepsilon$ ) as:  $\sigma=K\varepsilon^n$ , where  $K$  is the strength coefficient and  $n$  is the work-hardening exponent. Higher strain-hardening rate usually indicates better formability at room temperature [13,14]. The  $n$  values of the two samples were 0.12 along RD, 0.13 along TD for sample A; 0.27 along RD and 0.24 along TD for sample B, respectively. For metal sheets with good formability, such as Al and steel,  $n$  is typically about 0.20–0.50 at room temperature [15]. According to Ref. [16],  $n$  values of AZ31 and AM30 magnesium alloy sheets were 0.14 and 0.17, respectively. While for most magnesium alloys,  $n$  value is lower than 0.2. The  $n$  value of sample B in this work is well above most magnesium alloys, which exhibits better formability at room temperature.

It can be concluded that the  $\theta$  of sample A is higher than that of sample B in the linear hardening stage (stage II) along both RD and TD. And in stage III the work hardening rate of sample A is lower than that of sample B along RD and TD. Meanwhile, the  $\theta$  of sample A shows faster drop than sample B in both stages II and III. The grain size refinement causes a strong decrease in the hardening rate and it is likely attributed to the

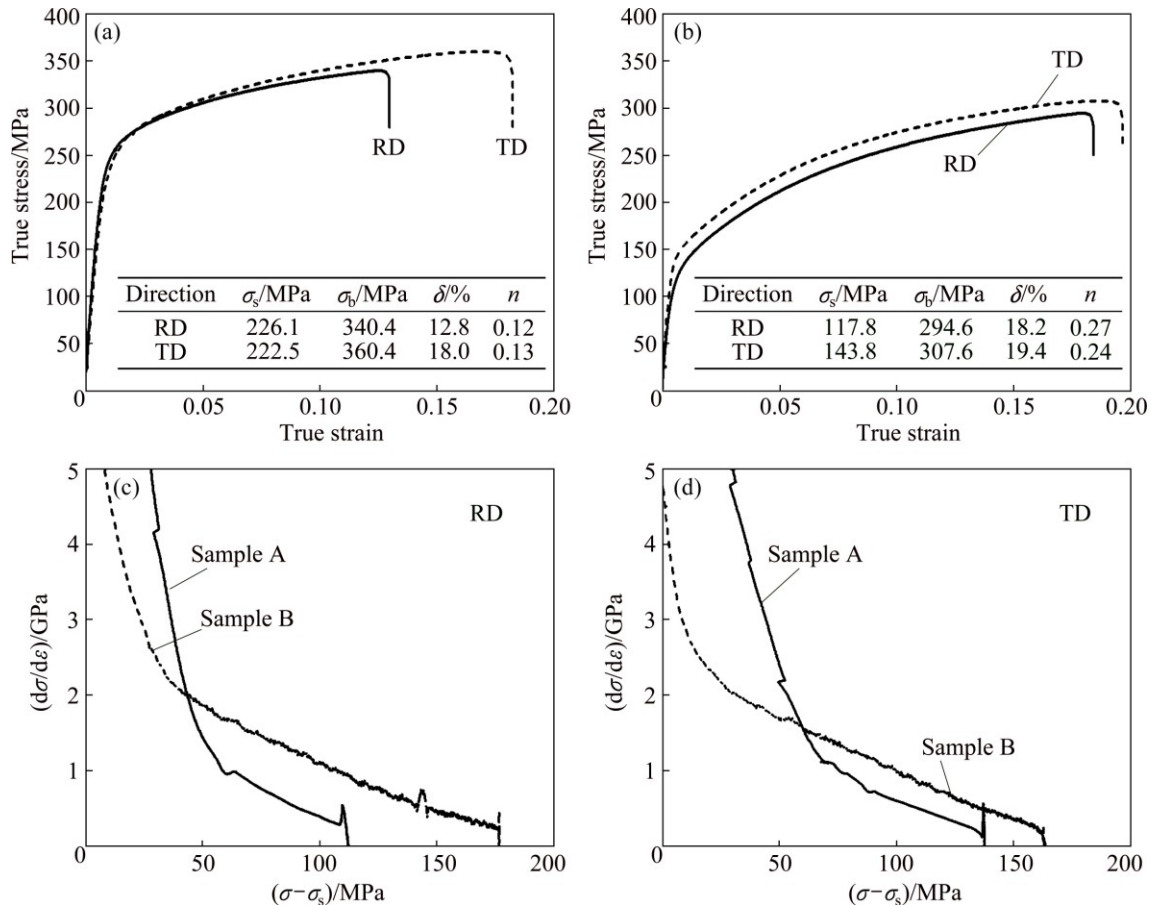


**Fig. 5** Room-temperature stress–strain curves for initial cold-rolled sheets of sample A (a), sample B (b), and room-temperature hardening curves of two samples along RD (c) and along TD (d)

contribution of grain boundary sliding to deformation [1]. A random texture was beneficial for higher ductility in magnesium alloy sheets at room temperature [17], which was due to the fact that the majority of grains in the weaker basal texture have an orientation favorable for dislocation glide on the basal plane [18]. As for the influence of twinning on work hardening, QIAO et al [19] reported that the number of twinning plays a minor role in work-hardening behaviors compared with grain size and texture.

For magnesium alloy, texture weakening is beneficial for the enhancement of the hardening capacity, which was due to the fact that the majority of grains in the weaker basal texture have an orientation favorable for dislocation glide on the basal plane [18]. The hardening ability of plastic procedure for sample B is far better than sample A, indicating that the basal slip is as the dominant. The more active basal slip and less active non-basal slip go against the generation of stress concentration, which is in favor of its compatible deformation, and then greatly improves the cold formability. Thus, the maximum single pass cold rolling reduction of sample A with strong texture was only 8% and sample B with weak texture state showed such good cold rolling formability. The one pass cold rolling reduction prior to failure of sample B was enhanced to 41%. When the reduction reached 51%, the as-rolled sheet generated edge cracks; however, on the surface of the sheet there was still good area as shown in Fig. 6. The cold formability of magnesium alloys was usually improved by adding rare earth elements to weaken texture. WU et al [20] examined the rollability and surface quality of AZ31 and GZ31 (Mg–3Gd–1Zn) magnesium alloy sheets. When rolled at the single-pass reduction larger than 10%, the AZ31 cold-rolled specimen undergoes significant surface cracking due to its strong basal texture. By contrast, the GZ31 cold-rolled sheet reveals a good surface without cracks observed on the surface or side margin, with the

single-pass reduction as high as 30%. By multi-pass rolling with small reduction (1%–5%) per-pass, the total reduction can reach 45% without the appearance of cracks. By contrast, AZ31 magnesium alloy sheet without cracks was obtained by single pass cold rolling at the reduction of 41% in this work.

## 4 Conclusions

1) Initial cold rolling sheet with good formability can be obtained by larger rolling reduction per pass during multi-pass hot rolling of AZ31 magnesium alloy sheet.

2) The maximum single pass cold rolling reduction of AZ31 magnesium alloy is greatly enhanced to 41%. Texture weakening is in favor of the improvement of hardening ability, and then affects the cold formability of AZ31 magnesium alloy sheet in spite of grain coarsening.

## References

- [1] DEL VALLE J A, CARRE O F, RUANO O A. Influence of texture and grain size on work hardening and ductility in magnesium-based alloys processed by ECAP and rolling [J]. *Acta Materialia*, 2006, 54: 4247–4259.
- [2] MUKAI T, YAMANOI M, WATANABE H, HIGASHI K. Ductility enhancement in AZ31 magnesium alloy by controlling its grain structure [J]. *Scripta Materialia*, 2001, 45: 89–94.
- [3] BARNETT M R, NAVE M D, BETTLES C J. Deformation microstructures and textures of some cold rolled Mg alloys [J]. *Materials Science and Engineering A*, 2004, 386: 205–211.
- [4] CHANG L L, SHANG E F, WANG Y N, ZHAO X, QI M. Texture and microstructure evolution in cold rolled AZ31 magnesium alloy [J]. *Materials Characterization*, 2009, 60: 487–491.
- [5] HUANG G S, XU W, HUANG G J, WANG L Y. Microstructure and mechanical properties of AZ31B magnesium alloy after cold rolling and annealing [J]. *Heat Treatment of Metals*, 2009, 5: 18–20.
- [6] LIU D, LIU Z Y, WANG E D. Effect of rolling reduction on microstructure, texture, mechanical properties and mechanical anisotropy of AZ31 magnesium alloys [J]. *Materials Science and Engineering A*, 2014, 612: 208–213.
- [7] PREZ-PRADO M T, DEL VALLE J, RUANO O A. Effect of sheet thickness on the microstructural evolution of an Mg AZ61 alloy during large strain hot rolling [J]. *Scripta Materialia*, 2004, 50: 667–671.
- [8] XIN Y C, WANG M Y, ZENG Z, HUANG G J, LIU Q. Tailoring the texture of magnesium alloy by twinning deformation to improve the rolling capability [J]. *Scripta Materialia*, 2011, 64: 986–989.
- [9] WANG Y N, CHANG C I, LEE C J, LIN H K, HUANG J C. Texture and weak grain size dependence in friction stir processed Mg–Al–Zn alloy [J]. *Scripta Materialia*, 2006, 55: 637–640.
- [10] AGNEW S, YOO M, TOME C. Application of texture simulation to understanding mechanical behavior of Mg and solid solution alloys containing Li or Y [J]. *Acta Materialia*, 2001, 49: 4277–4289.
- [11] WANG Y N, HUANG J C. Texture analysis in hexagonal materials [J]. *Materials Chemistry and Physics*, 2003, 81: 11–26.
- [12] GUO F, ZHANG D F, YANG X S, JIANG L Y, PAN F S. Microstructure and texture evolution of AZ31 magnesium alloy during large strain hot rolling [J]. *Transactions of Nonferrous Metals*

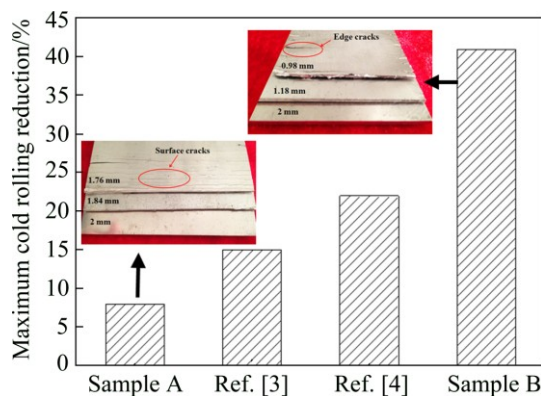


Fig. 6 Maximum cold rolling reduction of samples A and B in this work and Refs. [3,4]

- Society of China, 2015, 25: 14–21.
- [13] YAN H, CHEN R S, HAN E H. Room-temperature ductility and anisotropy of two rolled Mg–Zn–Gd alloys [J]. *Materials Science and Engineering A*, 2010, 527: 3317–3322.
- [14] ZHOU P, BEEH E, WANG M, FRIEDRICH H E. Dynamic tensile behaviors of AZ31B magnesium alloy processed by twin-roll casting and sequential hot rolling [J]. *Transactions of Nonferrous Metals Society of China*, 2016, 26: 2846–2856.
- [15] DUYGULU O, AGNEW S R. The effect of temperature and strain rate on the tensile properties of textured magnesium alloy AZ31B sheet [C]//*Magnesium Technology*, 2003. San Diego, CA, USA. TMS. 237–242.
- [16] LUO A A, SACHDEV A K. Development of a new wrought magnesium-aluminum-manganese alloy AM30 [J]. *Metallurgical and Materials Transactions A*, 2007, 38: 1184–1192.
- [17] CHINO Y, LEE J S, SASSA K, KAMIYA A, MABUCHI M. Press formability of a rolled AZ31 Mg alloy sheet with controlled texture [J]. *Materials Letters*, 2006, 60: 173–176.
- [18] AGNEW S R, HORTON J A, LILLO T M, BROWN D W. Enhanced ductility in strongly textured magnesium produced by equal channel angular processing [J]. *Scripta Materialia*, 2004, 50: 377–381.
- [19] QIAO Y D, WANG X, LIU Z Y, WANG E D. Effects of grain size, texture and twinning on mechanical properties and work-hardening behaviors of pure Mg [J]. *Materials Science and Engineering A*, 2013, 578: 240–246.
- [20] WU D, TANG W N, CHEN R S, HAN E H. Strength enhancement of Mg–3Gd–1Zn alloy by cold rolling [J]. *Transactions of Nonferrous Metals Society of China*, 2013, 23: 301–306.

## 控制初始织构提高 AZ31 镁合金板材 冷轧单道次变形量

刘迪, 刘祖岩, 王尔德

哈尔滨工业大学 材料科学与工程学院 金属精密热加工国家级重点实验室, 哈尔滨 150001

**摘要:** 利用多道次降温热轧工艺得到的 AZ31 镁合金板材用于后续的一道次冷轧实验, 单道次冷轧极限提高到 41%。在多道次降温热轧工艺中, 采用大的道次变形量进行轧制得到的终轧板材的织构强度较弱, 得到的织构强度仅为一般 AZ31 轧制板材的 1/3~1/2。研究表明, 即使得到的板材的晶粒尺寸较为粗大, 但是弱的织构仍有利于冷轧成形性的提高。对 AZ31 镁合金板材织构形成的变形机理进行了详细分析。

**关键词:** AZ31 镁合金; 织构控制; 冷成形性; 加工硬化

(Edited by Xiang-qun LI)